# Manuscript Details

**Manuscript number** AA_2017_572

**Title** Onsite vibrational characterization of DCMIX2/3 experiments

**Article type** Research paper

## Abstract

The SODI-DCMIX thermodiffusion series experiments are part of the fluid research program carried out by the European Space Agency on board of the International Space Station (ISS). In particular, DCIMIX2/3 were conducted in the past inside the Microgravity Science Glovebox in the US Laboratory. Due to the physical nature of the processes implied, these kind of runs were very long and particularly delicate because the low vibratory limit requirements must be maintained for hours. This restrictive condition not always is achieved, therefore, an accurate surveillance of the acceleration levels along the different experiments is necessary, to ensure a correct interpretation of the experimental results. This work analyzes onsite vibrational environment of DCMIX2/3 covering the periods in which the experiments were going on. To do so, acceleration signals only coming from the es03 sensor, nearest to the experimental equipment and located in the Glovebox, were downloaded from the PIMS NASA website. To be as precise as possible the signals have always been treated minute by minute. To detect the transient disturbances along the experiments, several warnings were considered. First, one minute RMS values, for the three acceleration components were evaluated, in time and in frequency domain. Additional information was obtained by plotting the power spectral densities of the signals, PSD, and their spectrogram with the aim of characterizing long periods of acceleration data. Due to great influence of low frequencies in this type of experiments, the Frequency Factor Index, FFI, was evaluated each minute. Complementary, the spectral entropy evolution was proposed as a fast new indicator of external perturbations. It has been found a good correlation between the spectrogram, temporal RMS and spectral entropy. Finally, a graphic representation of the points associated to the one-minute RMS values in one-third-octave frequency intervals which exceed the ISS limit curve requirements, was considered as a new and easy strategy for depicting the warnings that recognize the main disturbances along the experiment.

**Keywords** DCMIX; acceleration signal; ISS vibrational environment; spectral entropy

**Manuscript category** Space Physical Science

**Corresponding Author** Gavalda Josefina

**Order of Authors** Judit Ollé, Diana Dubert, Gavalda Josefina, Ana Laverón-Simavilla, Xavier Ruiz, Valentina Shevtsova

**Suggested reviewers** Tatyana Lyubimova, Jean Claude legros

# Submission Files Included in this PDF

**File Name [File Type]**

cover letter.pdf [Cover Letter]

document.docx [Manuscript File]

Fig1.tif [Figure]

Fig2.tif [Figure]

Fig3.tif [Figure]

Fig4.tif [Figure]

Fig5.tif [Figure]

Fig6.tif [Figure]

Fig7I.tif [Figure]

Fig8.tif [Figure]

Fig9.tif [Figure]

Fig10.tif [Figure]

Fig11.tif [Figure]

UNIVERSITAT
ROVIRA I VIRGILI

DEPARTAMENT DE QUÍMICA FÍSICA
I INORGÀNICA

Campus Sescelades
Marcel·lí Domingo, s/n
43007 Tarragona
Tel. +34 977 55 81 37
Fax +34 977 55 95 63
www.quimica.urv.es

Tarragona, May 12th 2017

Dear editor,

Please find enclosed the paper entitled:

"Onsite vibrational characterization of DCMIX2/3 experiments" by J. Ollé et al. To be considered for publication in the Acta Astronautica Journal.

Sincerely,

Dra. Josefina Gavaldà
SPABE Group
University Rovira i Virgili
C/Marcel.li Domingo s/n , 43007 Tarragona (SPAIN)

# Onsite vibrational characterization of DCMIX2/3 experiments

Judit Ollé[a], Diana Dubert[a], Josefina Gavaldà[a*], Ana Laverón-Simavilla[b], Xavier Ruiz[a,c] and Valentina Shevtsova[d]

[a] Departament Química Física i Inorgànica, Universitat Rovira i Virgili. Tarragona, Spain.
[b] E-USOC. ETSIAE, Universidad Politécnica de Madrid. Madrid. Spain.
[c] Institut d'Estudis Espacials de Catalunya, IEEC. Barcelona. Spain.
[d] Department of Chemical Physics, MRC, Université Libre Bruxelles, Belgium.
*Corresponding author: fina.gavalda@urv.cat

## Abstract

The SODI-DCMIX thermodiffusion series experiments are part of the fluid research program carried out by the European Space Agency on board of the International Space Station (ISS). In particular, DCIMIX2/3 were conducted in the past inside the Microgravity Science Glovebox in the US Laboratory. Due to the physical nature of the processes implied, these kind of runs were very long and particularly delicate because the low vibratory limit requirements must be maintained for hours. This restrictive condition not always is achieved, therefore, an accurate surveillance of the acceleration levels along the different experiments is necessary, to ensure a correct interpretation of the experimental results.

This work analyzes onsite vibrational environment of DCMIX2/3 covering the periods in which the experiments were going on. To do so, acceleration signals only coming from the es03 sensor, nearest to the experimental equipment and located in the Glovebox, were downloaded from the PIMS NASA website. To be as precise as possible the signals have always been treated minute by minute. To detect the transient disturbances along the experiments, several warnings were considered. First, one minute RMS values, for the three acceleration components were evaluated, in time and in frequency domain. Additional information was obtained by plotting the power spectral densities of the signals, PSD, and their spectrogram with the aim of characterizing long periods of acceleration data. Due to great influence of low frequencies in this type of experiments, the Frequency Factor Index, FFI, was evaluated each minute. Complementary, the spectral entropy evolution was proposed as a fast new indicator of external perturbations. It has been found a good correlation between the spectrogram, temporal RMS and spectral entropy. Finally, a graphic representation of the points associated to the one-minute RMS values in one-third-octave frequency intervals which exceed the ISS limit curve requirements, was considered as a new and easy strategy for depicting the warnings that recognize the main disturbances along the experiment.

**Keywords:** DCMIX, acceleration signal, ISS vibrational environment, spectral entropy

## 1. Introduction

DCMIX2/3 are the acronyms of two thermodiffusion experiments funded by the European Space Agency (ESA) and carried out recently in the ISS [1-3]. These experiments were proposed with the aim to obtain the values of Soret coefficients in case of ternary liquid mixtures under convection-free conditions. The values obtained in terrestrial laboratories can be, in this way, validated with the results generated in this microgravity environment. DCMIX2 was conducted from December 2013 until January 2014. The composition of the liquid mixture was toluene, methanol and cyclohexane (T-M-CH) and the runs (50 in total) were performed with cells containing the mixture at different concentrations. The selection of this ternary system is a consequence of some interesting features: such as the existence of an immiscibility gap in the ternary diagram and a wide region in which the Soret coefficients are negatives [4]. DCMIX3 experiments lasted from September until November 2016 and the ternary system focused on analysing aqueous mixtures such as water, ethanol and triethylene glycol, at different compositions, (total runs 31). All DCMIX2 and DCMIX3 runs were of long duration. The duration of DCMIX3 runs was 22 hours while the DCMIX2 experiment consisted of short and long runs (22h or less and 31.5 h, respectively). All the above experiments were held in thermodiffusive cells located in the SODI instrument which is installed in the Microgravity Science Glovebox (MSG) inside the U.S. Destiny module [5 -8].

Though the International Space Station (ISS) allows an environment with low-levels of acceleration, due to the very long time of both thermodiffusion experiments it is difficult to maintain ideal conditions along the runs. Daily crew activity, dockings, berthings and reboostings produce strong disturbances that are transmitted mechanically throughout the ISS structure [9-14]. The above disturbances could affect the ISS microgravity mode operation, ranging from $1x10^{-5}$ $m/s^2$ at low-frequencies to $1x10^{-1}$ $m/s^2$ at higher frequencies [9], [15,16]. In order to ensure that this mode is accomplished, the ISS disposes of different sensors of acceleration, namely MAMS (Microgravity Acceleration Measurement System) and SAMS (Space Acceleration Measurement System) situated in different locations inside the ISS modules which cover frequency ranges from less than 0.01 Hz (quasi-steady range) up to 300 Hz (vibratory range) [17-19]. The Principal Investigator Microgravity Services (PIMS) is the responsible for collecting all this information [20].

The objective of this work is, thus, to carry out an exhaustive study of the vibratory conditions during the DCMIX2/3 campaigns, analyzing the acceleration data provided by the es03 sensor which is the closest one to the experimental equipment in both cases. Notice however that, during DCMIX2 runs execution the sensor was located in the Ceiling Plate of the MSG, while that during DCMIX3 the location of the sensor moved to the rear wall of the MSG. The conclusion of this study is to detect possible disturbances that might affect the experimental measurements during the runs. However it must be cautious because a positive pulse-like detection does not always mean that the experimental measures must mandatorily be affected by the perturbation. In this sense, when processing the results of DCMIX2 it was found that some images had different types of perturbations. The analysis of the acceleration signals has identified that the experimental disturbances were caused by the optical system and not by the on-board g-jitter [21]. On the contrary, the analysis of the acceleration data of DCMIX3 allowed to identify an acceleration spike as the cause of sudden image shift in the interferometer (see Fig 1) [22]. In any case, the existence of a sufficient, but not necessary, relation between experimental perturbation and acceleration disturbances makes undoubtedly important the consideration of the accelerometric environment as a complementary factor to be simultaneously considered as, at least, warnings for the experimenter.

## 2. Numerical procedures

The acceleration signals analysed come from the SAMS es03 sensor which, located inside the MSG near the experiment, has a sampling rate of 250 Hz and a cutoff frequency of 101.4 Hz. Signals have been downloaded from the NASA Principal Investigator Microgravity Services, PIMS, website as binary files [13]. Data units are in g (9.8m/s$^2$) and before any mathematical manipulation, all raw signals have been systematically demeaned. In this work, the acceleration components always refer to the absolute coordinates of the International Space Station, ISS [23].

In order to accurately detect possible oscillatory disturbances during the DCMIX experiments, the signals were segmented in k records of 1 minute each. This interval has been considered as the basis of each warning in both time and frequency.

### 2.1 Time domain warnings

The one-minute interval root-mean-square (RMS) of acceleration has been estimated for each segment and for each acceleration component. This value gives an indication of the oscillation magnitude of the signal each minute. The RMS of the ax component and for the k segment, has been evaluated as follows [24]:

$$RMSax_k = \sqrt{\frac{1}{M}\sum_{i=1}^{M} ax^2} \quad (1)$$

where M is the number of the points in segment k.

Same expressions have been applied for the other acceleration components, ay and az. Based on the RMS of all three components one can evaluate a global RMS related with the module of the acceleration as follows:

$$RMS_k = \sqrt{RMSax_k^2 + RMSay_k^2 + RMSaz_k^2} \quad (2)$$

Time domain warnings are associated with the spikes of this last global RMS. Notice that the consideration of warnings in this way loses the information associated with the directionality of the perturbation. In all cases, a spike will be considered if its RMS value exceeds the 20% of the mean of all RMS values of the signal.

## 2.2. Frequency domain warnings

Frequency domain analyses were based on the power spectral density, PSD, estimated by the Welch method. As it is well known, this method splits the signals into overlapping windowing segments, calculates the periodogram of each one of them and finally averages the results to produce the final power spectral density [24, 25]. In this work we studied the PSD temporal evolution associated with the three acceleration components $a_x$, $a_y$ and $a_z$ taking also into account its minute by minute spectrogram.

In order to evaluate minute by minute the PSD intensity for a specific interval of frequency (f<1Hz or f<20Hz) with respect to the maximum PSD intensity of the whole frequency range, the frequency factor index function, FFI, for a selected record k has been defined as:

$$FFI(f)_k = log\frac{Max(PSD_k)}{PSD_k(f)} \qquad (3)$$

where $PSD_k(f)$ means the relative maximum power of the spectral density for a specific interval frequency and $Max(PSD_k)$ represents the absolute maximum value for all the frequency range. In this way, $FFI(f)_k$ try to condense in only one number the global relevance of the corresponding frequency interval minute by minute. Positive FFI values indicate that a low impact of the particularly dangerous low frequency band in the results of the experiment could be expected. Despite FFI is a time function, a unique value has finally been compiled in Tables for each run. This indicator has been obtained averaging the mean values of the three FFI functions associated with the three components of acceleration.

Based on the PSD evaluation and using the Parseval theorem, the one-minute RMS level, integrated over each one of the one-third octave bands, was also calculated for each component and for the module of the acceleration [20,21]. In particular, for the component ax, this value is computed as:

$$RMSax_j = \sqrt{\sum_{i=flow_j}^{i=fhigh_j}(PSDax(i))\Delta f} \qquad (4)$$

where Δf represents the frequency resolution in the evaluation of the PSD magnitude; *fhigh*$_j$ and *flow*$_j$ are the minimum and maximum frequency values in the j frequency band, and are calculated by the expressions:

$$flow_j = 0.1 * 2^{\left(\frac{j-1}{3}\right)} * 2^{\left(-\frac{1}{6}\right)} \quad (5)$$

$$fhigh_j = 0.1 * 2^{\left(\frac{j-1}{3}\right)} * 2^{\frac{1}{6}} \quad (6)$$

Identical expressions were used to calculate the RMS for the other two acceleration components, ay and az. Notice that the RMS is typically plotted together with a stair line, representing the International Space Station vibratory limit requirements [26] defined by:

$0.01 \leq f \leq 0.1 Hz$; $RMS \leq 1.8\ \mu g$ (7.a)

$0.1 < f \leq 100 Hz$; $RMS \leq 18 * f\ \mu g$ (7.b)

$100 < f \leq 300 Hz$; $RMS \leq 1800\ \mu g$ (7.c)

where *f* is the frequency in Hz. In the present case, as the cut off frequency is 101.4 Hz, the third limit level has not been taken into account.

Mention finally that global frequency warnings have been, as in time domain, based on the module of the acceleration of the whole signal. In this sense and in a similar way as in time warnings, frequency band warnings loosed the information associated with the directionality of the perturbation.

Finally, based on Shannon entropy concept [27], the analysis of the signal's entropy has been proposed with the aim of describing the degree of dispersion of their spectral energy using only a scalar. Moreover, with the help of this scalar, we can study the uniformity of the spectral distribution all along the experiment. A high value of the entropy, roughly unity, means that the energy spectrum is distributed meanwhile a low value, of the order of zero, indicates that the energy is concentrated only in a group of frequency bands. A change in entropy values expresses, thus, a redistribution of the spectrum energy.

The spectral entropy, $SEN_f$, was defined here based on the normalized power spectral density for each acceleration component, P, as follows:

$$SEN_f = -\frac{\sum_f P_f \left(log P_f\right)}{\log\left(N\right)} \quad (8)$$

where N is the number of discrete frequencies and P is the normalized power spectral density of each acceleration component. This power spectrum has been obtained over records of one minute, thus it is possible to plot the evolution of the $SEN_f$ entropy all along the DCMIX2/3 experiments. This magnitude constitutes a new tool to detect disturbances during an experiment allowing to study the regularity of the power spectral density distribution in time for a specific signal. Notice that a particularly advantageous feature of spectral entropy is that one can explicitly separate contributions from different frequency ranges in order to observe specific alterations of these ranges. The present work has concentrated in two of them, the first one containing all the frequencies (from 0.01 up to 100 Hz) and the second interval focusing on the lower frequencies (< 20 Hz).

## 3. Results

DCMIX2 consisted of 50 runs, though only 22 have been studied, due to some unpredictable inconveniences: lack of SAMS's data records, bubbles in the mixture or sensor data failure. In the case of DCMIX3 there were a total of 31 runs, but only 30 have been considered here. The one rejected presented incomplete data records. All these incidences are summarized in Table 1.

To illustrate the procedures used, only two representative signals have been presented and exhaustively discussed. The results concerning the rest of the signals are compiled in Tables 3 and 4. The first signal corresponds to the DCMIX2 run 7, conducted on December 8th, 2013, thereafter Run7_2, while the other matches the DCMIX3, run 20a performed on October 20th, 2016, thereafter Run20a_3. Remark that, Run 7_2 lasted for 31.5 hours while Run20a_3 only lasted 22 hours.

Figs 2.a and 2.b show the 1-minute interval RMS acceleration components for Run7_2 and Run20a_3, respectively. These values give a measure of the variation of the ax, ay and az acceleration components and immediately visualize gross changes in the acceleration levels caused by strong Station disturbances. It can be detected significant spikes for the three components of the Run7_2 signal around 1 hour and 25 hours, more pronounced in the $x_A$ direction. On the other side, the Run20a_3, Fig. 2.b shows more stable RMS values along all three acceleration components. In addition, Fig. 3 presents the 1-minute interval RMS values associated with the module of the acceleration for the same signals. The spikes detected in Fig 2 for both runs, have been enhanced now in this Figure. A thorough study on possible sources of these disturbances has been performed. It was found that during the DCMIX3 run, between 9:30 and 12:30 hours, a Soyuz MS-02/48S docking in the zenith port of the Poisk module occurred (see Table 2), but its influence in the RMS acceleration is negligible mainly in the $x_A$ direction, perpendicular to the docking one, (see Fig.2. b and Fig.3. b). In the case of DCMIX2 no extra activity was reported in the literature, thus the origin of the present spikes is, for the authors, unknown (see Table 2). A summary of the results obtained for the rest of signals are assembled as time domain warnings in Tables 3 and 4.

The power spectral densities for the three components of Run7_2 together with their spectrograms are displayed in Fig. 4. It can be seen that the highest PSD intensity for all three components is always located at 73.1 Hz. In general, it is well known that large frequency values are usually related to machinery operation, in this case the strong peak at 73.1 Hz can be attributed to the Glovebox fan in open mode [17]. This mode searches to extract the heat generated by the experiment itself maintaining a constant temperature. All three spectrograms detail a low frequency band (< 20 Hz) with moderate activity levels, showing some “discontinuities” along the experiment. This band concentrates the maximum values in an interval from 4 Hz to approximately 15 Hz, for $x_A$ and $y_A$ coordinates and it is shifted for the $z_A$ one (between 10 Hz-16 Hz). Fig. 5 plots the PSD and the spectrogram of the Run20a_3. The peak at 73.1 Hz, found in DCMIX2 experiments, also governs the power distribution of DCMIX3 trials. Moreover, the high frequencies (50-100 Hz) increased their intensity compared to the former case. At this respect, notice that, the sensor location inside the MSG, for each case, is different. This fact may have some influence in the general power distribution. At low frequencies (< 20 Hz), the PSD maximum values are more concentrated in a narrow band (12-17 Hz) compared to the Run7_2 which presents a broader one. The above narrow band is not always “continuous” but is similar for all three coordinates, unlike the first experiment. For years, the literature has shown special interest in identifying the disturbances present in the spectrograms. Due to this, many frequencies have been classified, though, there are still quite a few with unknown origin. A short summary of these findings could relate crew activity with frequency bands below 10 Hz, Ku-Band antennas influences between 5-30 Hz and general machinery (pumps, blowers, fans, etc.) working at higher frequencies [28,29]. Based on the literature, the present frequency bands detected, might thus be linked to the crew activity disturbances and general machinery functioning.

It is known that the low frequencies can disturb the thermodiffusive phenomena [30], so that, FFI of each acceleration component has been evaluated, for each experiment, with the aim of complementing the power distribution at lowest frequencies (see Fig. 6 and Fig. 7). Two intervals have been taken into account: frequency values less than 20 Hz and less than 1 Hz, respectively. The maximum PSD intensity of these two intervals was compared to the maximum frequency peak of 73.1 Hz found in Fig. 4 and 5, for both signals. Regarding Run7_2, the FFI values at frequencies < 20 Hz are maintained practically constant (around 3) for all three coordinates and along the entire time. In contrast, for frequencies < 1 Hz the FFI values oscillate with a period of around 10 hours, reaching higher values (approximately 5.5) in the middle of the run. FFI values (roughly 2.5 for frequencies < 20 Hz and around 4.5 for frequencies < 1 Hz) have also been obtained for Run20a_3 for both intervals. Remark that, FFI evaluated for frequencies < 20 Hz, presents more oscillatory behaviour with a characteristic period of approximately 1.5 hours, probably due to the rotation of the ISS around the Earth. For frequencies < 1 Hz, similar tendency with respect to Fig. 6, was detected, however, the wider interval (~10 h) appears at the beginning of the experiment. In these particular cases the FFI indicators are 3.0 (frequencies< 20 Hz) and 4.8 (frequencies< 1 Hz) for Run7_2 and 2.7 (frequencies< 20 Hz) and 4.5 (frequencies< 1 Hz) for Run20a_3, respectively. The FFI values for the rest of DCMIX2/3 signals are shown in Tables 3 and 4.

Fig. 8 plots the SEN values for the three acceleration components of the Run7_2, together with the spectrogram of the acceleration component in the $z_A$ direction. From this Figure, it can be seen that SEN values for low frequency range are always greater than the ones calculated for all frequency range. Moreover, these values are practically constant along the experiment. SEN values obtained for whole range of frequencies presents some spikes that could be used as indicators of possible modifications of the PSD distribution along the experiment substituting/complementing the classical spectrogram. Furthermore, comparing the Figs. 2.a and 8 it can be seen that the rise of the RMS values appear at the same times when the spikes in SEN were calculated for the whole range of frequencies. Furthermore, a good correlation has been obtained between the above spikes and the disturbances detected with the spectrogram (Fig.8 c and d). Analysing the other two coordinates, $x_A$ and $y_A$, similar constant SEN values in time were estimated for the low frequency interval and comparable spikes values (in case of all frequency range), indicating different disturbances in time were as well correlated with the corresponding RMS values and their spectrogram. Overall, Fig.8 and Fig.2a confirm the utility of SEN as a fast indicator for the detection of possible disturbances in time when all the frequency range is considered. Similar results were reached analysing the signal from the Run20a_3 (see Fig 9). It is remarkable that just one spike was present at around 17h of trial, in the $y_A$ and $z_A$ coordinates. This spike is not associated with the above mentioned Soyuz docking because it occurred between 10 and 13 h after starting the experiment equivalently between 7:30-10:30 h, October 21th 2016. It should be mentioned finally that the warnings extracted before from the RMS values fit very well with the warnings calculated using SEN values based on all the frequency range.

The RMS acceleration components in one-third-octave frequency intervals were calculated for intervals of 1 minute. As an example, Fig 10.a displays the RMS values for the minute 498 (8.3 hours) and is compared to the ISS limit requirements, in the vibratory range. This selected minute is plotted as a dashed line in Fig 10.b. It can be seen that RMS values are quite close to the limit curve crossing it at frequency ranges between 1.5 and 10 Hz for the all three acceleration components. Considering $x_A$ direction, the interval centred at 0.5 Hz also exceeds the limit curve. For frequencies lower than 0.5 Hz and higher than 10 Hz, for all the acceleration coordinates, the RMS values accomplishes perfectly with the ISS requirements. The points in time and frequency that overcame the microgravity mode condition during the entire experiment, may be considered as visual warnings and are summarized in Fig. 10.b. The microgravity mode condition is always accomplished for frequencies above 10 Hz, while at smaller ones the limit is surpassed during the most of the experiment. Fig 11.a shows the RMS acceleration components in one-third-octave frequency intervals for the Run20a_3 calculated in the minute 727 (12.11 hours). In this case, the three RMS values also overpass the limit requirements curve at low frequencies intervals (< 13 Hz). At high frequencies the RMS values follow the ISS requirements. The summarized warnings in both time and frequencies are plotted in Fig.11.b. The microgravity mode condition is accomplished perfectly by RMS values at frequencies higher than 13 Hz, meanwhile the low frequency RMSs (< 13 Hz) exceed this limit for entire run, except a specific interval between 4-8h. The graphic representation of the points exceeding the ISS limits (see Fig.10.b and Fig.11.b) could help in identifying easier and faster possible potentially dangereuses disturbances that might have a great effect on the ongoing experiments. Global frequency warnings based on the module of the acceleration of the whole signals are presented in Tables 3 and 4.

## Conclusions

A detailed analysis of the vibratory environment of the DCMIX2 and 3 runs was carried out minute by minute using acceleration signals coming from the nearest sensor to the experimental device (es03).

The evolution of RMS values in time clearly shows that there are some runs that are very stable, without any significant disturbances, while there are others that at quick glance show spikes that could provoke alterations in the thermodiffusion results. The 73.1 Hz dominates the PSD results for all three components considered and for both experiments. Usually, this frequency is associated to the Glovebox Fan in open mode. Similar broad band in the PSD for all coordinates and the two experiments, was detected at low frequencies (<20 Hz), though it presents lower PSD intensity. To quantify this intensity range, the Factor Frequency Index was calculated for frequency intervals less than 1 Hz and 20 Hz. The FFI values for both experiments and all three coordinates oscillated between 4.5 and 5 for the first interval. Analyzing the second frequency interval (< 20 Hz), the FFI values were slight higher (~ 3) for Run7_2 compared to Run20a_3 (~ 2.5). A better visualization of the band stability in time was obtained through the spectrogram. It can be seen that at high frequencies the PSD intensity is maintained along the run while at low frequencies some clear oscillation in the intensity occurred. In the case of the Run7_2 the broad band appeared in the low frequency interval differ from one coordinate to another. For the Run20a_3 this band seems to coincide for all the three coordinates. This behavior might be due to the different location of the sensor in the two experiments.

As mentioned above, in order to study the regularity of the power distribution in time for a specific signal, Spectral Entropy values were calculated for two different frequency intervals. The SEN results, for the both experiments and all three coordinates, indicated high punctual values (up to 0.7 – Run7_2 and 0.55 – Run20a_3) if the all frequencies interval is assumed. These values correlate perfectly with the spikes detected when RMS have risen, or with disturbances identified by the spectrogram. Considering the low frequency interval, SEN values detected no significant spikes in time, preserving a constant behaviour along the entire experiment. In other words, SEN as a tool for detecting possible disturbances in time, works better if the complete frequency interval is considered.

The points in time and frequency that were identified earlier as warnings, gathered crucial information regarding disturbances concentrated in the low frequency ranges, for both experiments. Considering frequencies higher than 13 Hz the microgravity mode condition is always accomplished, and no warnings were discovered. This RMS warning map is very useful in identifying easier and faster the possible disturbances in each experiment.

Overall, this article summarizes old and new techniques used to characterize different experiments, with the aim of keeping an accurate observation of the acceleration levels along these experiments and to ensure a correct interpretation of their results.

## Acknowledgments

We acknowledge the total support offered by Dr. W. Köhler and the PhD student T. Triller of the Physics Department, University of Bayreuth, Germany . We also acknowledge the constant support offered by Dr. K. Hrovat (ZIN Technologies, Inc.). This work was supported by the Spanish Ministerio de Economia y Competitividad, MINECO, grant number ESP2014-53603-P and by of the Generalitat de Catalunya, grant number, 2014SGR365

## References

[1] M. Lappa, C. Piccolo, G. Esposito, S. La Gala, D. Sorrentino, D. Giordano, G. De Chiara, G. Di Constanzo, R. Fortezza, C. Albanese, The SODI diffusion Soret Coefficient experiment onboard ISS: a flexible and modular approach to operations in orbit. Proceedings of the 63rd IAF International Astronautical Congress, Naples 2012.

[2] 〈https://www.nasa.gov/mission_pages/station/research/experiments/712.html〉.

[3] V. Shevtsova, measurements Soret and diffusion coefficients on the ISS. 42th COSPAR Assembly, Moscow Russia, (2014).

[4] V. Shevtsova, C. Santos, V. Sechenyh, J.C. Legros and A. Mialdun, Diffusion and Soret In ternary mixtures. Preparation of the DCMIX2 experiment on the ISS, Microgravity Sci. technol. 25 (2014) 275-283.

[5] D. A. de Mezquia, M. Larrañaga, M. M. Bou-Ali, J. A. Madariaga, C. Santamaría, J. K. Platten, Contribution to thermodiffusion coefficients measurements in DCMIX Project, Int. J. Therm. Sci., 92 (2015) 14-16.

[6] A. Mialdun and V. Shevtsova, Communication: New approach for analysis of thermodiffusion coefficients in ternary mixtures, J. Chem. Phys. 138 (2013) 161102.

[7] A. Mialdun, J.-C. Legros, V. Yasnou, V. Sechenyh and V. Shevtsova, Contribution to the benchmark for ternary mixtures: Measuremnt de Soregt, diffusion and thermodiffusion coefficients in the ternary mixture THN/IBB/n$C_{12}$ with 0.8/0.1/0.1 mass fractions in ground and orbital laboratories, Eur. Phys. J. E 38: 27 (2015).

[8] A. Mialdun and V. Shevtsova, Development of optical digital interferometry technique for measurement of thermodiffudsion coefficients, Int. J. Heat Mass Trans 51(2008) 3164-3178.

[9] B.V. Tryggvason, R.F. Redden, R.A. Herring, W.M.B. Duval, R.W. Smith, K.S. rezkallah, S. Varma, The vibration environment on the International Space Station: its significance to fluid-based experiments, Acta Astronaut. 48 (2-3) (2001) 59-70.

[10] R. DeLombard, K. Hrovat, E. Kelly, B. Humphreys, Interpreting the International Space Station microgravity environment, in: Proceedings of the 43rd AIAA Aerospace Sciences Meeting and Exhibit (ASME), Reno, Nevada 2005 (AIAA-2005-0727).

[11] N. Sáez, X. Ruiz, Jna. Gavaldà, J. Pallarés, V. Shevtsova, Comparative ISS accelerometric analyses, Acta Astronaut. 94 (2014) 681-689.

[12] N. Sáez, X. Ruiz, Jna. Gavaldà, V. Shevtsova, Comparative Analyses of ESA, NASA and JAXA signals of acceleration during the SODI-IVIDIL experiment, Microgravity Sci Tech. 26 (2014) 57-64.

[13] N. Sáez, Jna. Gavaldà, X. Ruiz, V. Shevtsova, Detecting accelerometric nonlinearities in the International Space Station, Acta Astronaut. 103 (2014) 16-25.

[14] R. Jurado, Jna. Gavaldà, M.J. Simón, J. Pallarés, A. Laverón-Simavilla, X. Ruiz, V. Shevtsova, Some considerations on the vibrational environment of the DSC-DCMIX1 experiment onboard ISS, Acta Astronaut. (2016).

[15] K. Jules, K. McPerson, K. Hrovat, E. Kelly, T. Reckart, A status report on the characterization of the microgravity environment of the International Space Station, Acta Astronaut. 55 (2004) 335-364.

[16] K. Jules, K. McPerson, K. Hrovat, E. Kelly, Initial characterization of the microgravity environment of the international space station: increments 2 through 4, Acta Astronaut. 55 (2004) 855-887.

[17] NASA, Pims Nasa Handbook, 2013. URL

⟨http://pims.grc.nasa.gov/pimsdocs/public/ISS%20Handbook/hb_vib_equipment_MSG_Operations.pdf⟩.

[18] McPherson, K., Keller, J., Kelly, E., Hrovat, K.: The NASA Glenn Research Center/s acceleration measurement and analysis projects support for the International Space Station (ISS), ASTRO2012, 16th CASI astronautics conference. Quebec City, Canada (2012)

[19] Heese, J., Moss, L.: ISS payload microgravity control and disturbance predictions. Microgravity Environment interpretationTutorial (MEIT), Section 19, pp 1–67 (2004)

[20] ⟨https://pims.grc.nasa.gov/html/ISSAccelerationArchive.html⟩.

[21] A. Mialdun and V. Shevtsova, Temperature dependence of Soret and diffusion coefficients for toluene–cyclohexane mixture measured in convection-free environment, J. Chem. Phys. 143 (2015), 224902.

[22] W. Köhler and T. Triller, The DCMIX3 campaign of the ESA/Roscosmos DCMIX project, News Letters of ELGRA, 10 (2016) 10.

[23] K. Jules, K. Hrovat, E. Kelly and T. Reckart, International Space Station Increment 6/8 microgravity environment. Summary report (2005). NASA/TM-2005-213896.

[24] M.J.B. Rogers, K. Hrovat, E. Kelly, T. Reckart, Accelerometer data analysis and presentation techniques, NASA Lewis Research Center, Clevehand, Ohio, 1997.

[25] Hrovat, K.: Analysis techniques for vibratory data, NASA 7th Annual Microgravity Environment Interpretation Tutorial, NASA Glenn Research Center. Ohio Aerospace Institute, Cleveland, Ohio, 2004.

[26] Jules, K.: Working in a reduced-gravity environment: “A Primer/”,Microgravity Environment Interpretation Tutorial (MEIT),Section 2, pp. 1–77 (2002)

[27] C. E. Shannon, A mathematical theory of communication. Bell System Tech. J. 27(1948) 379.

[28] PIMS Microgravity Environment Handbook; http://pims.grc.nasa.gov/handbook

[29] K. McPherson, K. Hrovat, E. Kelly, J. Keller, A researcher’s guide to: International Space Station Acceleration Environment, NASA Report NP-2015-11-040-JSC, 2015.

[30] Y. Yan, V. Shevtsova, M.Z. Saghir, Numerical study of low frequency g-jitter effect on thermal diffusion, Fluid Dynamics and Material Processing Journal 1 (2005) 315-328.

## Figure captions

Fig 1. Experimental perturbation and the corresponding acceleration spike. (Source: T. Triller, W. Köhler, DCMIX3b – firsts results, Topical Team Meeting, Bruxelles, 2017 ).

Fig 2 One-minute interval RMS for the three acceleration components: a) Run7_2 and b) Run20a_3.

Fig. 3 One-minute interval RMS acceleration vector: a) Run7_2 and b) Run20a_3.

Fig. 4 Power spectral density and spectrogram of Run7_2 of: a) the acceleration component in the $x_A$ direction, b) the acceleration component in the $y_A$ direction and c) the acceleration component in the $z_A$ direction.

Fig 5 Power spectral density and spectrogram of the Run20a_3 acceleration components: a) $x_A$ direction, b) $y_A$ direction and c) $z_A$ direction.

Fig 6 Frequency Factor Index, FFI, evolution for the two frequency intervals considered and for the Run7_2 acceleration components: a)in the $x_A$ direction, b)in the $y_A$ direction and c) in the $z_A$ direction.

Fig 7 Frequency Factor Index, FFI, evolution for the two frequency intervals considered and for the Run20a_3 acceleration components: a) in the $x_A$ , b) in the $y_A$ and c) in the $z_A$ direction, respectively.

Fig. 8 SEN evolution for all frequency domain an for frequencies < 20Hz associated to the Run7_2 acceleration components: a) in the $x_A$ direction, b) in the $y_A$ direction and c) in the $z_A$ direction.

Fig. 9 SEN evolution for all frequency domain an for frequencies < 20Hz associated to the Run20a_3 acceleration components: a) in the $x_A$ direction, b) in the $y_A$ direction and c) in the $z_A$ direction.

Fig. 10 Run7_2: a) RMS acceleration components vs. one third octave frequency bands calculated in the 498 minute 498. b) Marks indicating when the RMS acceleration components exceeds the ISS Limit curve requirements.

Fig. 11 Run20a_3: a) RMS acceleration components vs. one third octave frequency bands calculated in the 727 minute. b) Marks indicating when the RMS acceleration components exceeds the ISS Limit curve requirements.

Table 1: DCMIX2/3 incidences

| **Incidence** | **DCMIX2** | | **DCMIX3** | |
|---|---|---|---|---|
| SAMS problems | Run 1 | Cell 1 | Run 1 | Cell 1 |
| | Run 2 | Cell 2 | | |
| | Run 3 | Cell 3 | | |
| | Run 33 | Cell 1 | | |
| | Run 31 | Cell 3 | | |
| | Run 4 | Cell 4 | | |
| | Run 18 | Cell 3 | | |
| Aborted experiments | Run 1bis | Cell 1 | - | - |
| | Run 10 | Cell 5 | | |
| | Run 25 | Cell 4 | | |
| | Run 30 | Cell 3 | | |
| Bubbles | Run 2s | Cell 2 | - | - |
| | Run 2s2 | Cell 2 | | |
| | Run 2s3 | Cell 2 | | |
| | Run 2s4 | Cell 2 | | |
| | Run 0s1 | Cell - | | |
| | Run 4s1 | Cell 4 | | |
| | Run 2s5 | Cell 2 | | |
| | Run 0s2 | Cell - | | |
| | Run 4s2 | Cell 4 | | |
| | Run 29 | Cell 4 | | |
| | Run 0s3 | Cell 0 | | |
| | Run 3s1 | Cell 3 | | |
| | Run 4s3 | Cell 4 | | |
| | Run 5s1 | Cell 5 | | |
| | Run 0s4 | Cell 0 | | |
| | Run 2s6 | Cell 2 | | |
| | Run 3s2 | Cell 3 | | |
| Without incidences | 22 runs | | 30 runs | |

Table 2: Main disturbances during the period of activity of the DCMIX2/3 experiments.

| Experiments | Date | Spacecraft type | Port | Disturbance | | Remarks |
|---|---|---|---|---|---|---|
| | | | | Kind | Main direction | |
| DCMIX2 (01/12/2013-24/01/2014) | 11/12/2013 | Progress M-21M/53P | Aft port of the Svezda's module | Reboosting | $+X_A$ | No run |
| | 13/12/2013 | Progress M-21M/53P | Aft port of the Svezda's module | Reboosting | $+X_A$ | Cell 5, started at 08:54, but the run was aborted at 14:57 and run data was deleted |
| | 24/12/2013 | - | - | US EVA | - | No run |
| | 26/12/2013 | - | - | RS EVA | - | The EVA was done during the diffusion phase (cell 1), but the run data was completed |
| | 12/01/2014 | Cygnus CRS Orb-1 | Nadir port of the Harmony module | Berthing (Canadarm2) | $-Z_A$ | No run |
| | 18/01/2014 | Progress M-21M/53P | Aft port of the Svezda's module | Reboosting | $+X_A$ | No run |
| DCMIX3 19/09/2016-22/11/2016) | 21/10/2016 | Soyuz MS-02/48s | Zenith port of the Poisk module | Docking | $+Z_A$ | The docking was done during the thermodiffusion process (cell 5), but run data was completed |
| | 23/10/2016 | Cygnus CRS OA-5 | Nadir port of the Unity module | Berthing | $-Z_A$ | No run |
| | 03/11/2016 | Svezda's service module | - | Reboosting | $+X_A$ | The reboosting was done during thermalization (cell 2), but run data was completed |
| | 19/11/2016 | Soyuz MS-03 | Nadir port of the Rassvet module | Docking | $+Z_A$ | No run |
| | 23/11/2016 | Cygnus CRS OA-5 | Nadir port of the Unity module | Unberthing (Canadarm2) | $-Z_A$ | The unberthing was done during thermalization (cell 2), but run data was completed |

Table 3: Warnings of the complete DCIMX2 experiment.

| **Run** | **Cell** | **Run time** | **StartTime** | **EndTime** | **FFI (Freq.)** | | **Frequency domain warnings (Hz)** | **Time domain warnings*** |
|---|---|---|---|---|---|---|---|---|
| | | | | | **<20Hz** | **<1Hz** | | |
| 5 | 5 | 31.5h | 06/12/2013<br>5:15 | 07/12/2013<br>12:45 | 3.0 | 4.7 | - | 1:05:31<br>8:16:30<br>12:32:24<br>28:29:24 |
| 6 | 1 | 22h | 07/12/2013<br>12:45 | 08/12/2013<br>10:45 | 3.0 | 4.9 | - | Correct |
| 7 | 2 | 31.5h | 08/12/2013<br>10:45 | 09/12/2013<br>18:15 | 3.0 | 4.8 | 0-0.11 band | 0:54:29<br>23:29:24 |
| 8 | 3 | 22h | 09/12/2013<br>18:15 | 10/12/2013<br>16:15 | 3.0 | 4.7 | - | 17:26:24<br>17:39:39 |
| 9 | 4 | 31.5h | 12/12/2013<br>1:24 | 13/12/2013<br>8:54 | 2.8 | 4.7 | - | 13:11:24 |
| 11 | 1 | 22h | 13/12/2013<br>16:22 | 14/12/2013<br>14:22 | 2.8 | 4.8 | - | 21:53:24 |
| 10bis | 5 | 31.5h | 14/12/2013<br>14:23 | 15/12/2013<br>21:53 | 2.7 | 4.7 | - | 0:09:30 |
| 12 | 2 | 31.5h | 15/12/2013<br>21:54 | 17/12/2013<br>5:24 | 2.6 | 4.8 | - | 9:53:31<br>21:30:36 |
| 13 | 3 | 22h | 17/12/2013<br>5:24 | 18/12/2013<br>3:24 | 2.6 | 4.6 | 0.17-0.22 band<br>11.4-14.37 band | - |
| 14 | 4 | 31.5h | 18/12/2013<br>3:24 | 19/12/2013<br>10:54 | 2.7 | 4.7 | 0.17-0.22 band<br>11.4-14.37 band | - |
| 15 | 5 | 31.5h | 19/12/2013<br>10:54 | 20/12/2013<br>18:24 | 2.6 | 4.7 | 11.4-14.37 band | - |
| 16 | 1 | 22h | 26/12/2013<br>22:15 | 27/12/2013<br>20:15 | 2.7 | 4.5 | 0-0.11 band<br>0.22-0.28 band | 20:15:36<br>20:23:24<br>20:50:24<br>21:41:24 |
| 20 | 5 | 31.5h | 02/01/2014<br>13:26 | 03/01/2014<br>20:56 | 3.0 | 4.6 | 0.17-0.22 band | 20:22:12<br>29:09:36<br>29:31:12 |
| 19e | 4 | 31.5h | 03/01/2014<br>20:56 | 05/01/2014<br>4:26 | 3.0 | 4.5 | 0.11-0.14 band<br>0.17-0.22 band<br>0.28-0.35 band | 10:55:12<br>24:28:12 |
| 21 | 1 | 12h | 07/01/2014<br>11:12 | 07/01/2014<br>23:12 | 3.2 | 4.4 | 0.11-0.14 band<br>0.17-0.22 band<br>0.28-0.35 band | 3:37:30<br>4:18:28 |
| 22 | 3 | 12h | 07/01/2014<br>23:12 | 08/01/2014<br>11:12 | 3.1 | 5.0 | - | - |
| 23 | 4 | 17h | 08/01/2014<br>11:12 | 09/01/2014<br>4:12 | 3.2 | 4.8 | 0.11-0.14 band | - |
| 24 | 5 | 17h | 09/01/2014<br>4:13 | 09/01/2014<br>21:13 | 3.1 | 4.6 | 0.11-0.14 band | 11:07:12 |
| 26 | 1 | 22h | 09/01/2014<br>21:13 | 10/01/2014<br>19:13 | 3.0 | 4.9 | - | 16:51:36<br>18:03:36<br>18:41:24<br>19:57:36 |
| 27 | 3 | 22h | 14/01/2014<br>11:27 | 15/01/2014<br>9:27 | 3.1 | 4.9 | 3.59-4.53 band | 4:36:28 |
| 32 | 1 | 17h | 16/01/2014<br>14:47 | 17/01/2014<br>7:47 | 3.1 | 4.8 | 0-0.11 band | 3:37:30<br>3:54:28 |
| 28 | 5 | 31.5h | 20/01/2014<br>20:09 | 22/01/2014<br>3:39 | 2.5 | 4.6 | 0.17-0.22 band<br>11.4-14.37 band | 14:45:36<br>17:27:36<br>21:56:24 |

*Time has been calculated using t = 0 when the run started.

Table 4: Warnings of the complete DCIMX3 experiment.

| Run | Cell | StartTime | EndTime | FFI (Freq.) | | Frequency domain warnings (Hz) | Time domain warnings* |
|---|---|---|---|---|---|---|---|
| | | | | <20Hz | <1Hz | | |
| 5 | 5 | 19/09/2016 7:22 | 20/09/2016 5:22 | 2.7 | 4.7 | - | 8:29:18 |
| 4 | 4 | 20/09/2016 5:23 | 21/09/2016 3:23 | 2.8 | 4.8 | - | 4:03:51 |
| 2 | 2 | 21/09/2016 3:23 | 22/09/2016 1:23 | 2.9 | 4.9 | - | 7:45:39 |
| 1 | 1 | 22/09/2016 1:23 | 22/09/2016 23:23 | 2.9 | 5.0 | - | - |
| 10 | 5 | 22/09/2016 23:23 | 23/09/2016 21:23 | 3.0 | 5.0 | - | 09:43:54<br>19:13:54 |
| 9 | 4 | 26/09/2016 6:21 | 27/09/2016 4:21 | 3.0 | 4.8 | - | 08:49:38<br>11:59:38 |
| 6 | 1 | 27/09/2016 4:21 | 28/09/2016 2:21 | 3.0 | 4.9 | - | - |
| 3 | 3 | 28/09/2016 2:21 | 29/09/2016 0:21 | 3.0 | 4.8 | - | - |
| 14 | 4 | 29/09/2016 0:21 | 29/09/2016 22:21 | 2.8 | 4.9 | - | 11:32:02 |
| 7 | 2 | 29/09/2016 22:21 | 30/09/2016 20:21 | 2.7 | 4.8 | - | - |
| 15 | 5 | 04/10/2016 2:23 | 05/10/2016 0:23 | 2.9 | 4.8 | 0.08-0.11 band | 12:51:41 |
| 12 | 2 | 05/10/2016 0:23 | 05/10/2016 22:23 | 2.9 | 4.8 | - | - |
| 20 | 5 | 06/10/2016 20:23 | 07/10/2016 18:23 | 2.9 | 4.9 | - | 01:27:01 |
| 8 | 3 | 11/10/2016 6:59 | 12/10/2016 4:59 | 2.8 | 4.7 | - | 07:48:06<br>09:21:06 |
| 16 | 1 | 12/10/2016 4:59 | 13/10/2016 2:59 | 2.8 | 4.7 | - | - |
| 13 | 3 | 13/10/2016 2:59 | 14/10/2016 0:59 | 2.8 | 4.8 | 0.17-0.22 band | 12:37:41 |
| 19 | 4 | 18/10/2016 3:46 | 19/10/2016 1:46 | 2.6 | 4.8 | - | 10:49:05 |
| 18 | 3 | 19/10/2016 1:46 | 19/10/2016 23:46 | 2.6 | 4.7 | 0.11-0.14 band | 05:59:30<br>08:53:30<br>15:15:30 |
| 17 | 2 | 19/10/2016 23:46 | 20/10/2016 21:46 | 2.8 | 4.6 | 0.11-0.14 band | - |
| 20a | 5 | 20/10/2016 21:46 | 21/10/2016 19:46 | 2.7 | 4.5 | 0.11-0.14<br>0.17-0.22<br>1.1-1.4 bands | 16:51:48 |
| 21 | 4 | 27/10/2016 14:33 | 28/10/2016 12:33 | 3.0 | 4.7 | 0.11-0.14<br>3.5-4.5 bands | 00:42:12<br>02:42:12 |
| 22 | 2 | 02/11/2016 7:22 | 03/11/2016 5:22 | 3.2 | 5.1 | - | 08:48:14 |
| 23 | 1 | 03/11/2016 5:22 | 04/11/2016 3:22 | 3.2 | 5.0 | - | 03:25:22 |
| 24 | 5 | 07/11/2016 7:26 | 08/11/2016 5:26 | 3.1 | 4.9 | - | 13:38:42 |
| 25 | 2 | 08/11/2016 5:26 | 09/11/2016 3:26 | 3.1 | 4.8 | - | - |
| 26 | 4 | 09/11/2016 3:26 | 10/11/2016 1:26 | 3.1 | 4.9 | - | - |
| 27 | 5 | 15/11/2016 5:03 | 16/11/2016 3:03 | 2.8 | 4.9 | - | - |
| 28 | 1 | 16/11/2016 3:03 | 17/11/2016 1:03 | 2.9 | 4.9 | 0.08-0.11<br>5.7-7 bands | 13:40:54 |
| 29 | 4 | 17/11/2016 1:04 | 17/11/2016 23:04 | 2.9 | 4.9 | - | 14:59:02 |
| 30 | 2 | 22/11/2016 3:41 | 23/11/2016 1:41 | 3.1 | 4.7 | 0.08-0.11<br>0.22-0.28<br>bands | 3:26:37<br>6:54:37<br>9:17:37 |

*Time has been calculated using t = 0 when the run started.

# Notable Events

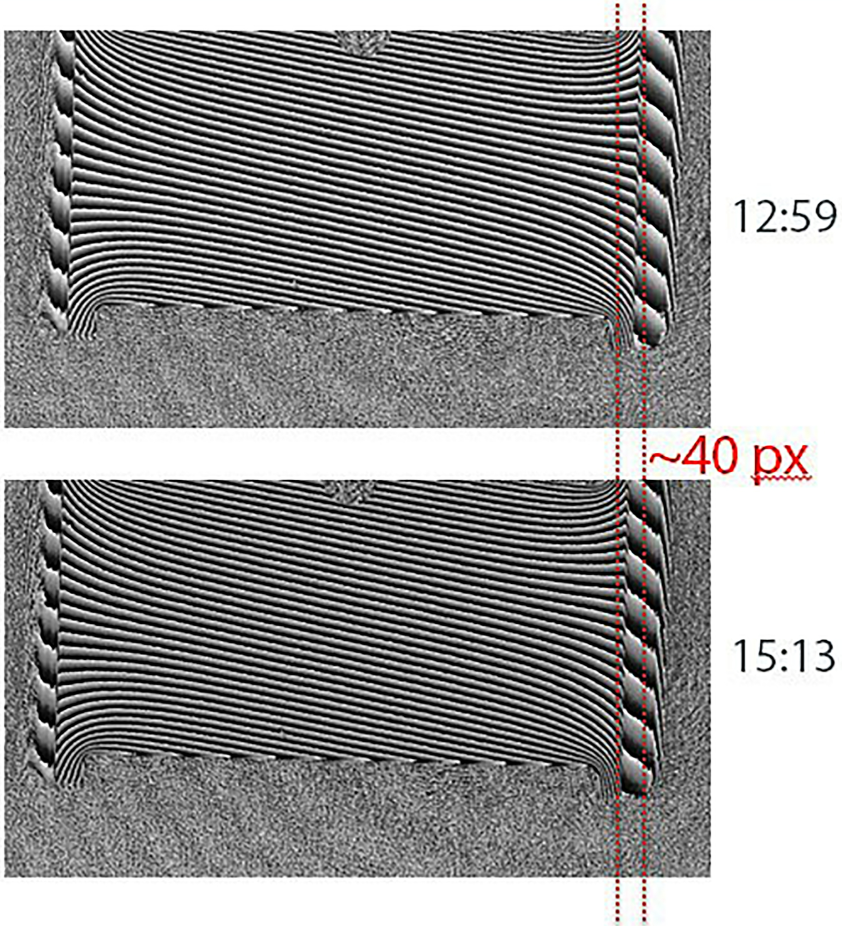

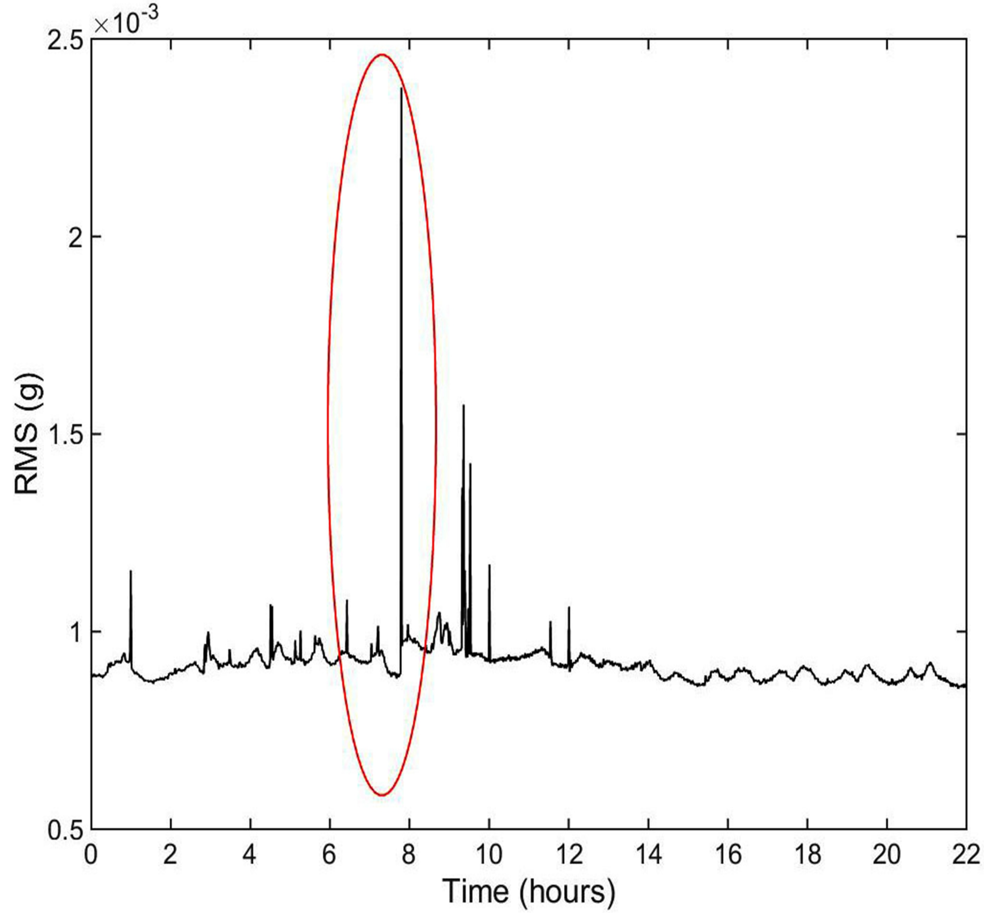

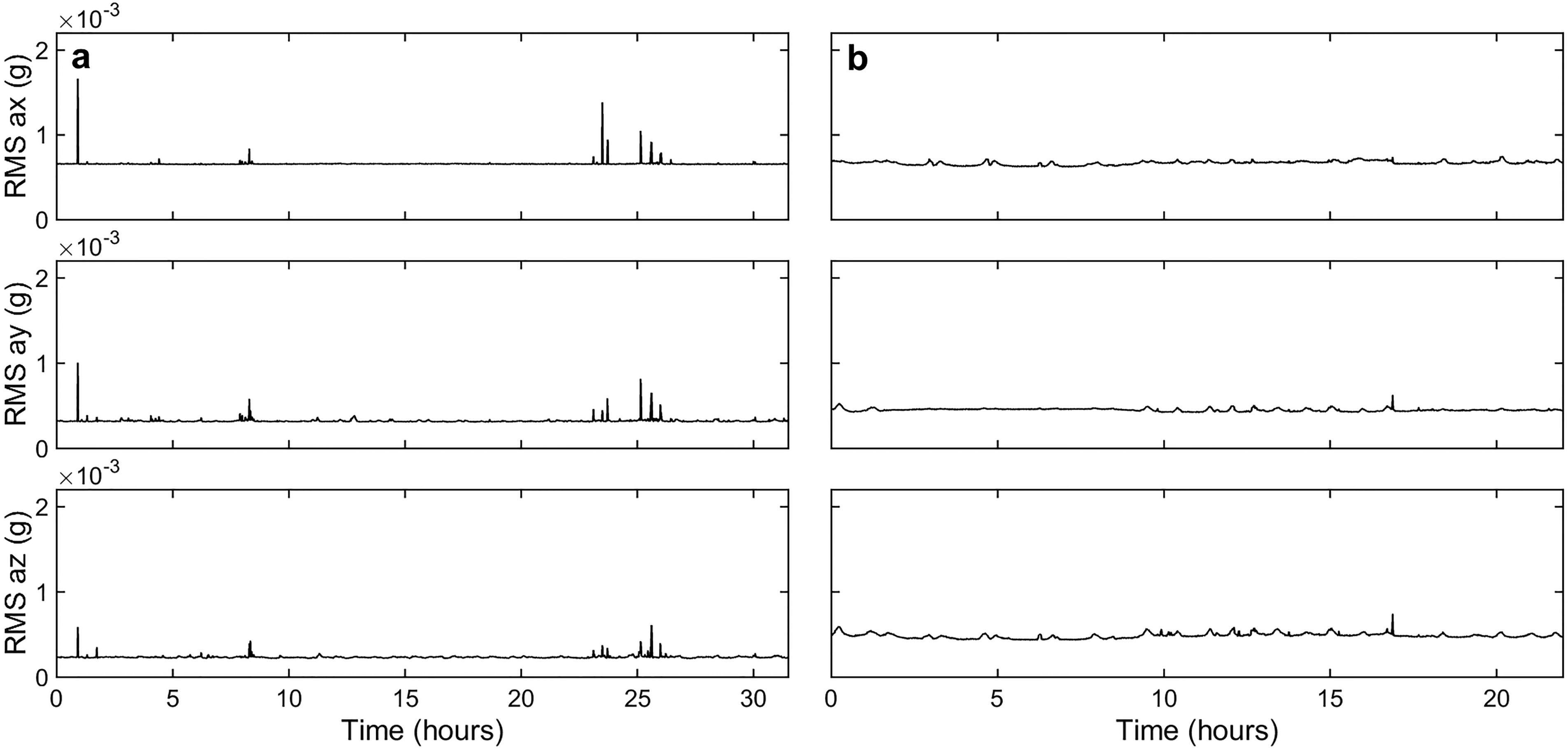
a
b
×10^-3
RMS ax (g)
RMS ay (g)
RMS az (g)
0
1
2
0
5
10
15
20
25
30
Time (hours)
0
5
10
15
20
Time (hours)

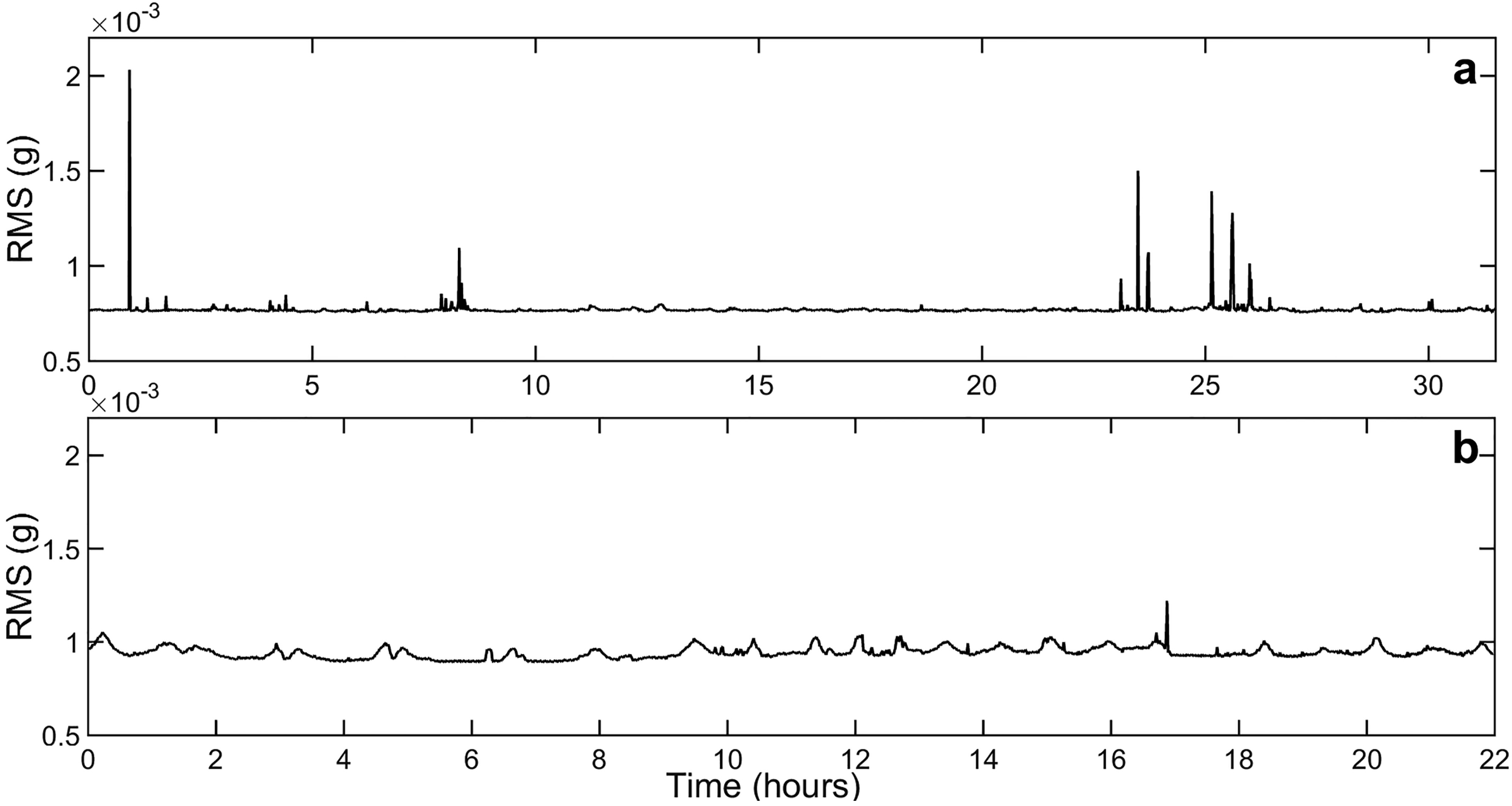
×10-3
a
RMS (g)
0.5
1
1.5
2
0
5
10
15
20
25
30
×10-3
b
RMS (g)
0.5
1
1.5
2
0
2
4
6
8
10
12
14
16
18
20
22
Time (hours)

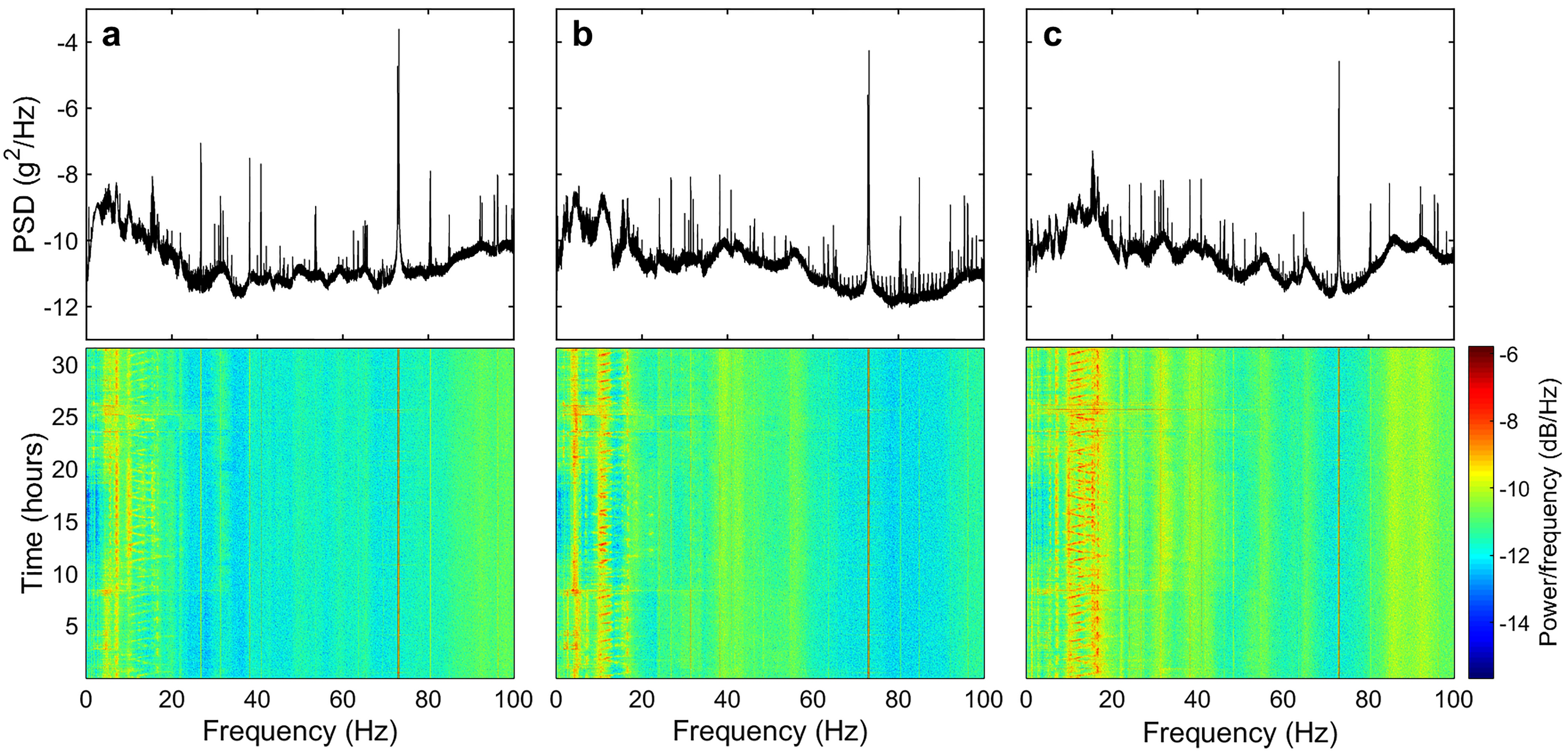
a
b
c
PSD (g$^2$/Hz)
-4
-6
-8
-10
-12
Time (hours)
30
25
20
15
10
5
0
20
40
60
80
100
Frequency (Hz)
Power/frequency (dB/Hz)
-6
-8
-10
-12
-14

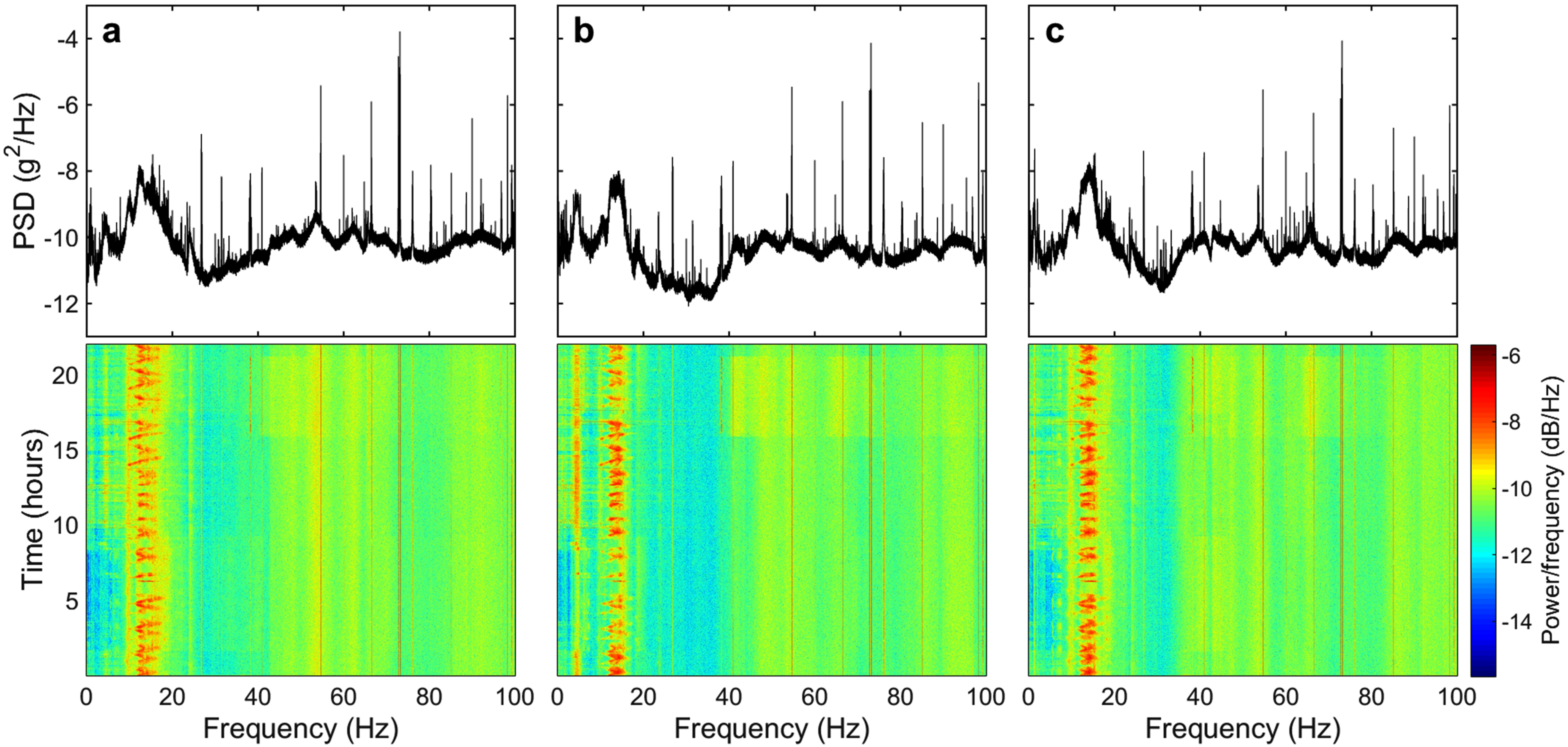
a
b
c
PSD (g$^2$/Hz)
-4
-6
-8
-10
-12
Time (hours)
20
15
10
5
0
20
40
60
80
100
Frequency (Hz)
Power/frequency (dB/Hz)
-6
-8
-10
-12
-14

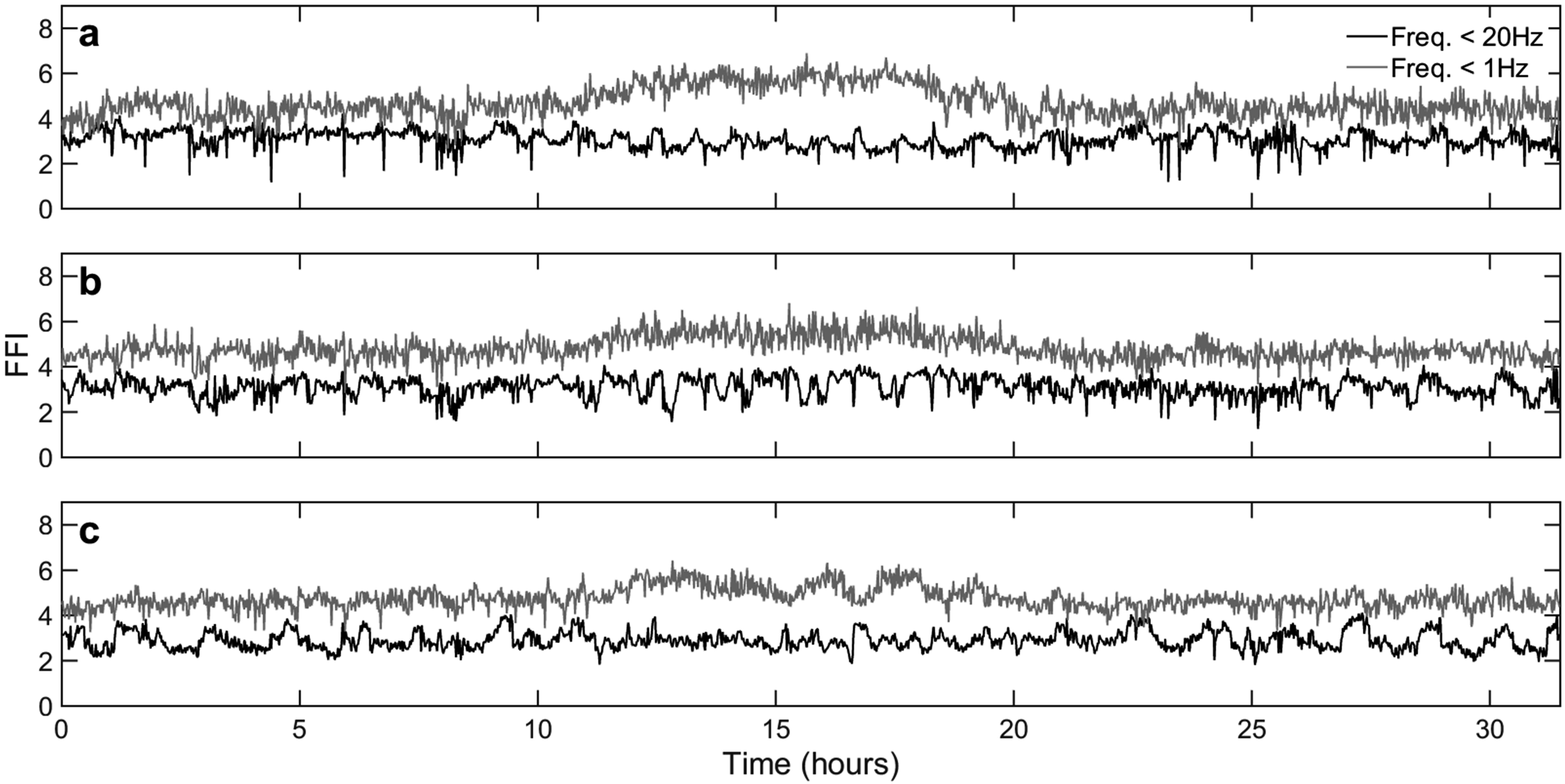
a
b
c
Freq. < 20Hz
Freq. < 1Hz
FFI
0
2
4
6
8
Time (hours)
0
5
10
15
20
25
30

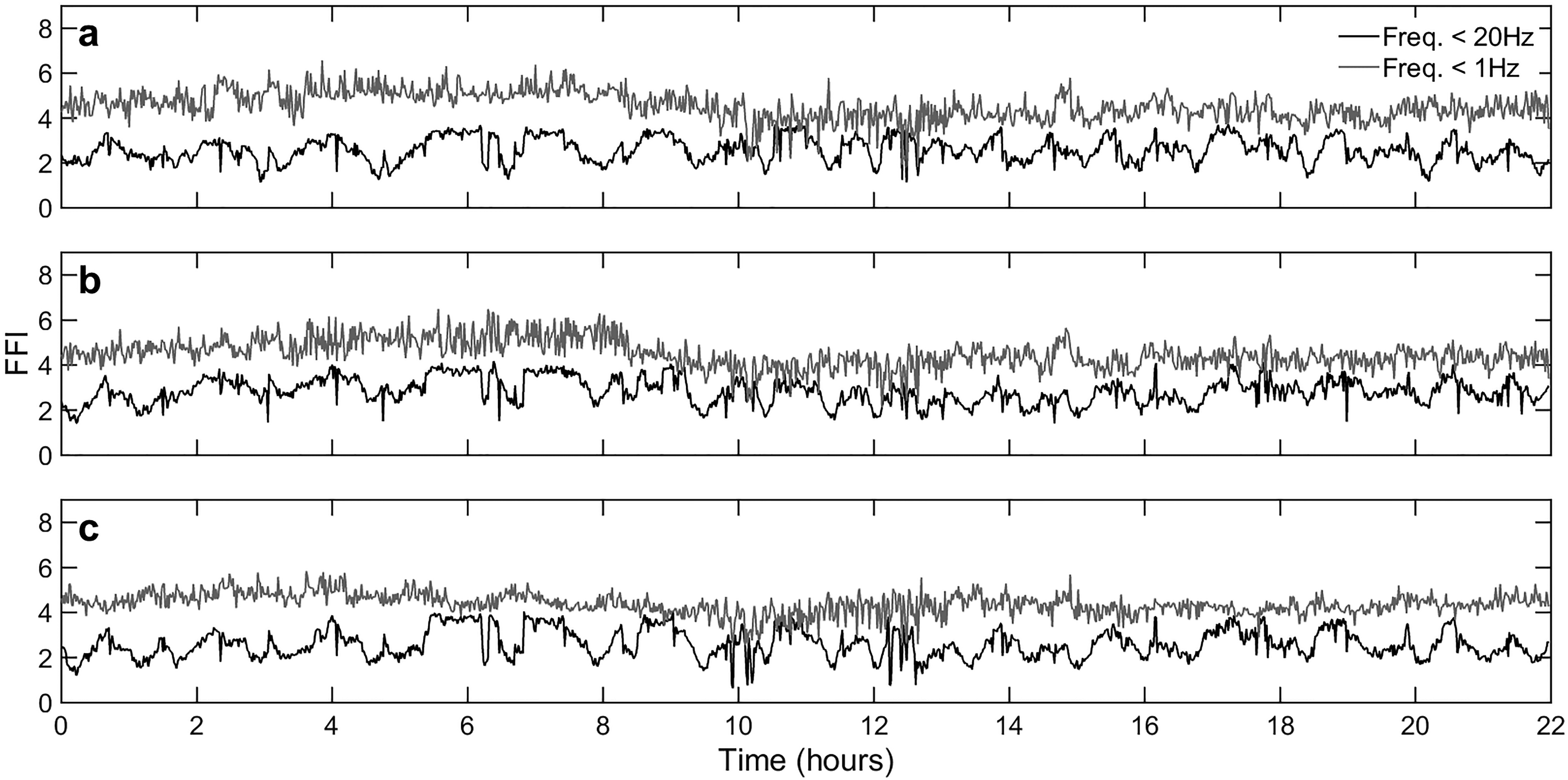
a
b
c
Freq. < 20Hz
Freq. < 1Hz
FFI
0
2
4
6
8
0
2
4
6
8
10
12
14
16
18
20
22
Time (hours)

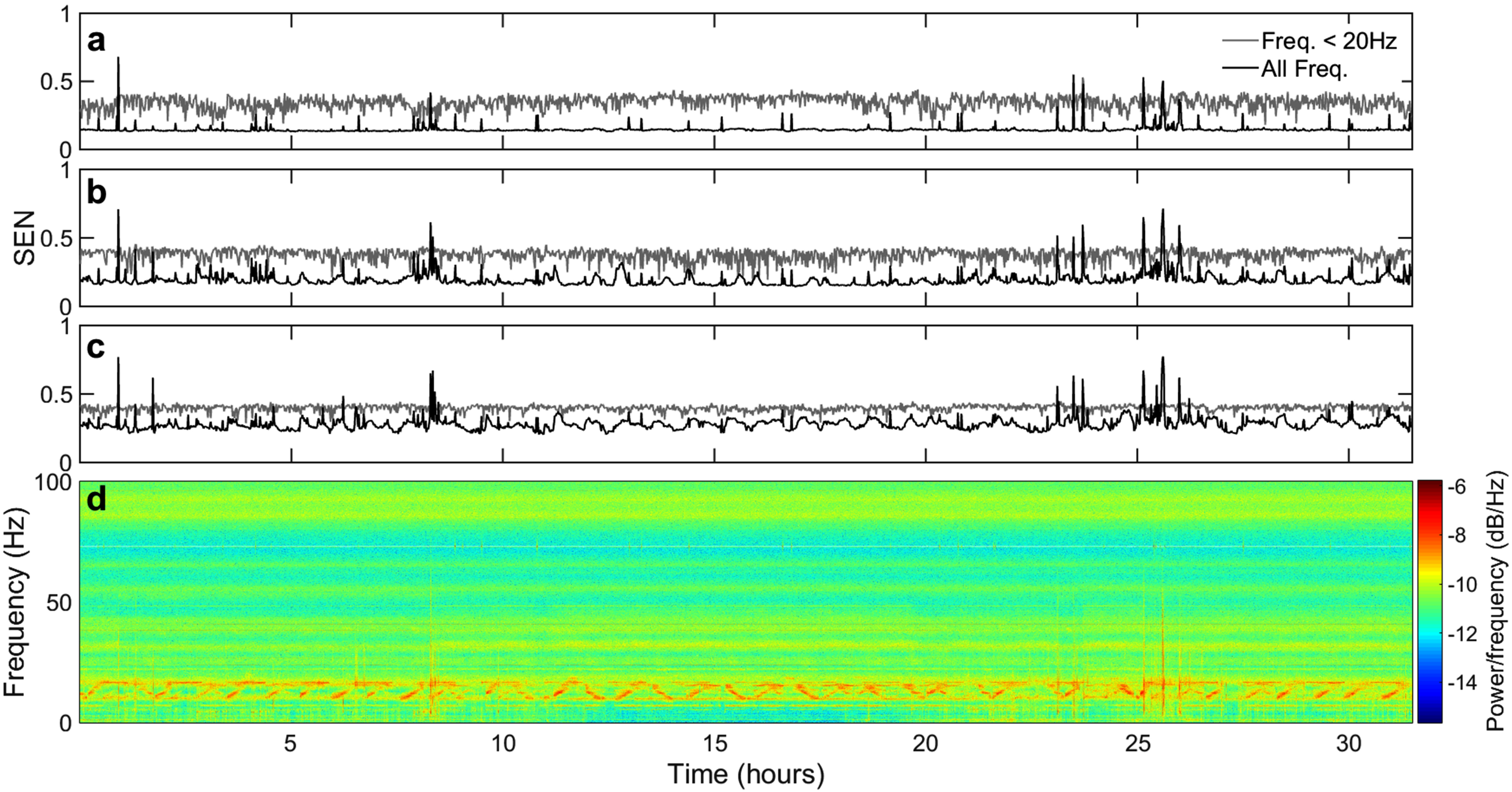
a
b
c
d
Freq. < 20Hz
All Freq.
SEN
1
0.5
0
100
50
Frequency (Hz)
5
10
15
20
25
30
Time (hours)
-6
-8
-10
-12
-14
Power/frequency (dB/Hz)

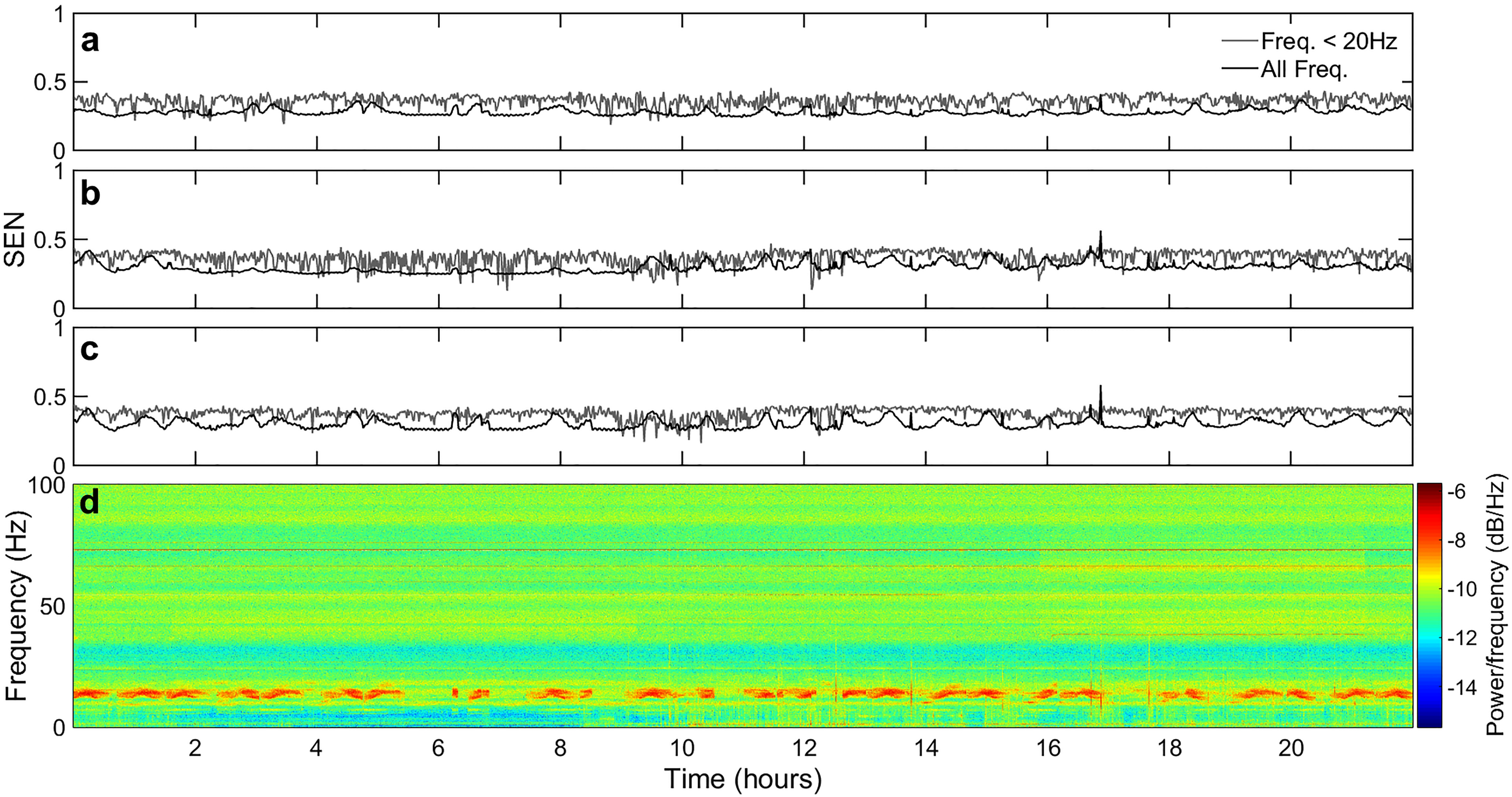
a
b
c
d
Freq. < 20Hz
All Freq.
SEN
1
0.5
0
Frequency (Hz)
100
50
0
2
4
6
8
10
12
14
16
18
20
Time (hours)
Power/frequency (dB/Hz)
-6
-8
-10
-12
-14

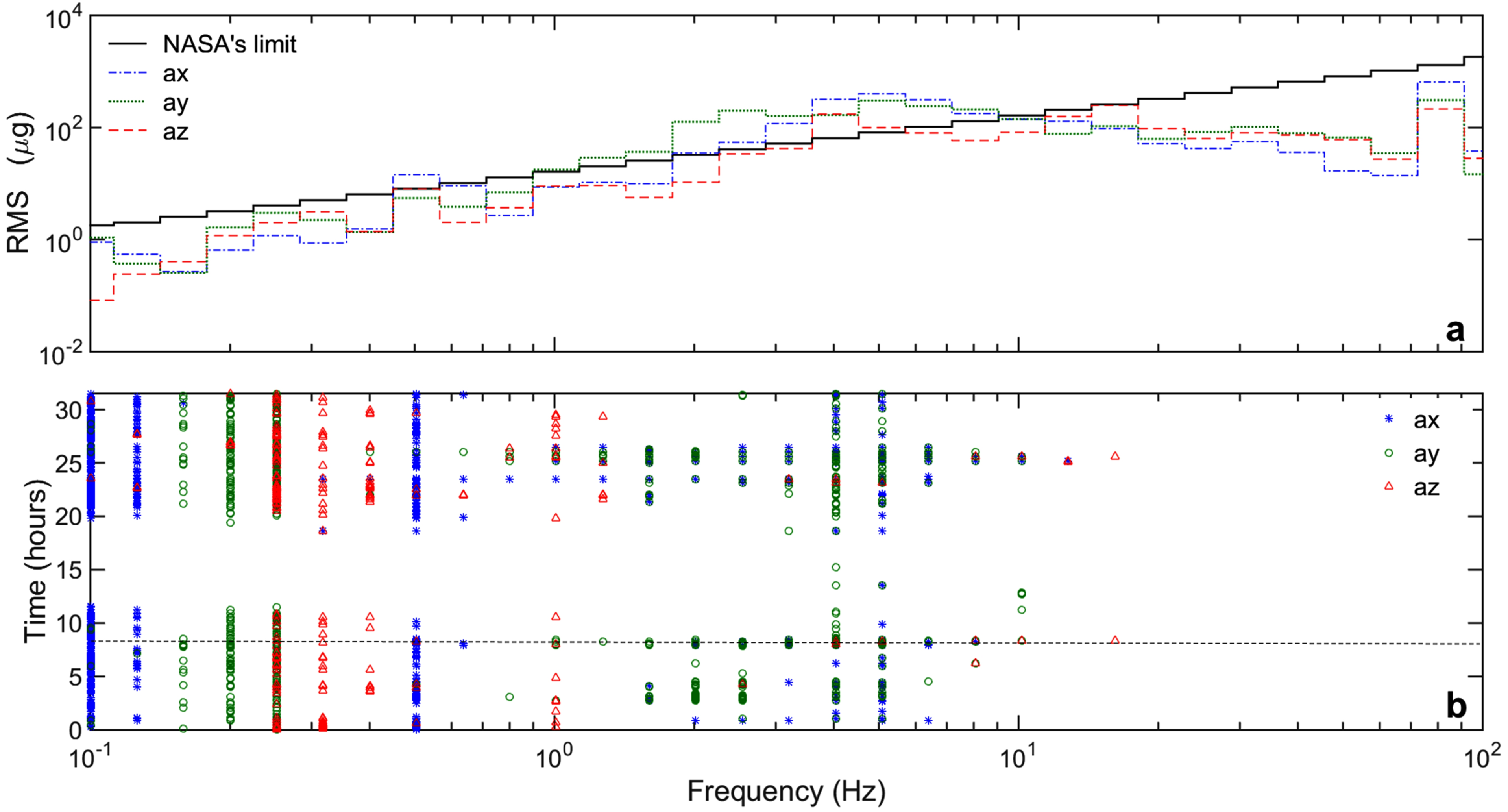
NASA's limit
ax
ay
az
RMS ($\mu$g)
$10^4$
$10^2$
$10^0$
$10^{-2}$
a
ax
ay
az
Time (hours)
30
25
20
15
10
5
0
b
$10^{-1}$
$10^0$
$10^1$
$10^2$
Frequency (Hz)

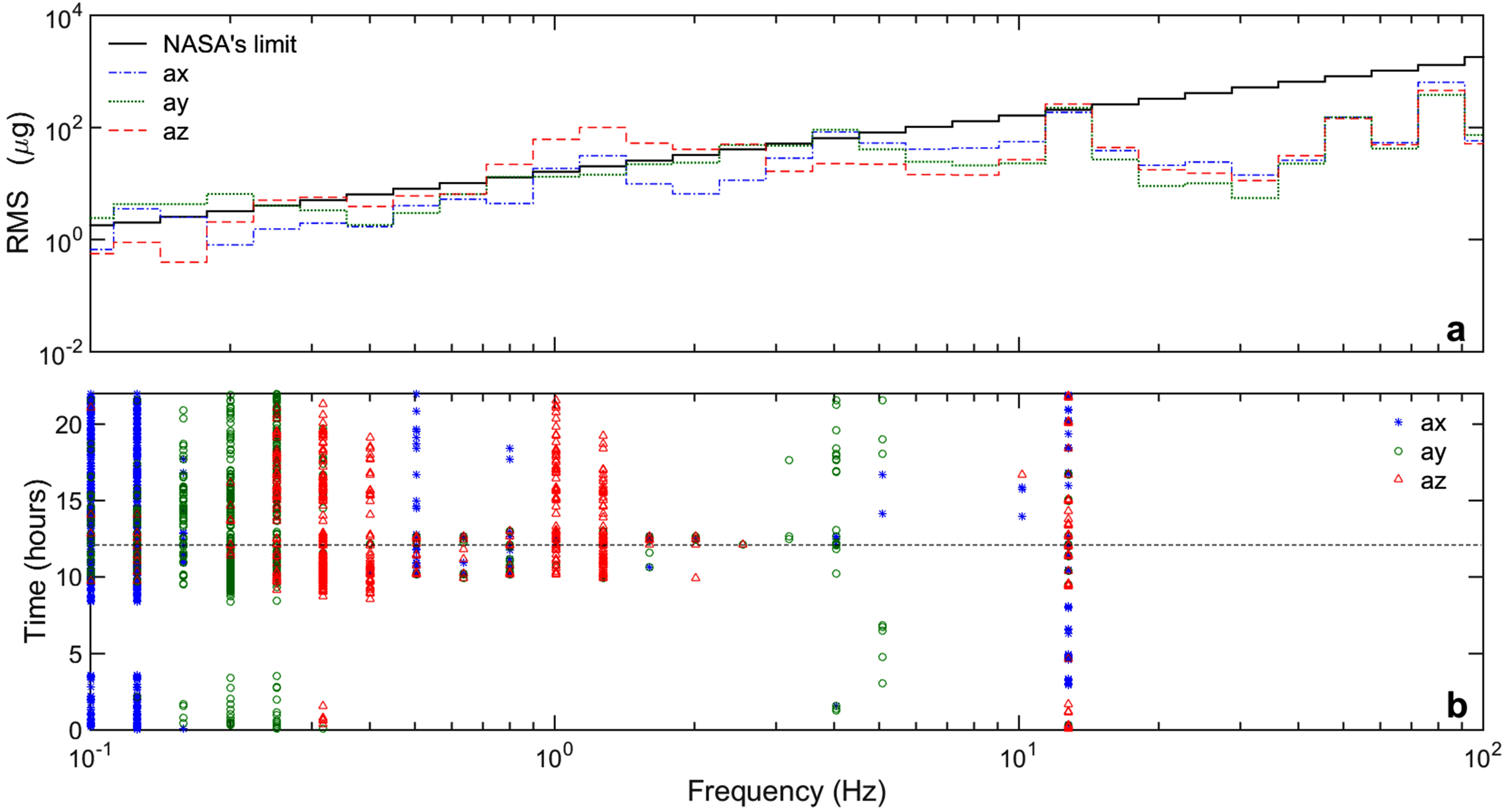
10^4
10^2
10^0
10^-2
RMS (μg)
NASA's limit
ax
ay
az
a
20
15
10
5
0
Time (hours)
ax
ay
az
b
10^-1
10^0
10^1
10^2
Frequency (Hz)